




ARTICLE

The stress-responsive gene *GDPGP1/mcp-1* regulates neuronal glycogen metabolism and survival

Alexander Schulz^{1,2} , Yuichi Sekine^{1,3} , Motunrayo J. Oyeyemi^{1,2}, Alexander J. Abrams^{1,2}, Manasa Basavaraju^{1,2}, Sung Min Han^{1,2}, Marco Groth⁴ , Helen Morrison⁴, Stephen M. Strittmatter^{2,3} , and Marc Hammarlund^{1,2} 

Maladaptive responses to stress might play a role in the sensitivity of neurons to stress. To identify novel cellular responses to stress, we performed transcriptional analysis in acutely stressed mouse neurons, followed by functional characterization in *Caenorhabditis elegans*. In both contexts, we found that the gene *GDPGP1/mcp-1* is down-regulated by a variety of stresses. Functionally, the enzyme *GDPGP1/mcp-1* protects against stress. Knockdown of *GDPGP1* in mouse neurons leads to widespread neuronal cell death. Loss of *mcp-1*, the single homologue of *GDPGP1* in *C. elegans*, leads to increased degeneration of GABA neurons as well as reduced survival of animals following environmental stress. Overexpression of *mcp-1* in neurons enhances survival under hypoxia and protects against neurodegeneration in a tauopathy model. *GDPGP1/mcp-1* regulates neuronal glycogen levels, indicating a key role for this metabolite in neuronal stress resistance. Together, our data indicate that down-regulation of *GDPGP1/mcp-1* and consequent loss of neuronal glycogen is a maladaptive response that limits neuronal stress resistance and reduces survival.

Introduction

Cells contain mechanisms to cope with altered physiological demands, to survive periods of intense stress, and to adapt to chronic stress (Vijayalaxmi et al., 2014). Successful adaptation to stressful conditions, such as hypoxia, involves changes in genetic programs that modulate metabolism, cell death, growth, and cellular differentiation (Mattson, 2008). But cells may also respond to stress in maladaptive ways. Such responses are those that limit the ability to withstand stress and so decrease survival. Identifying maladaptive neuronal stress responses is thus critical for a comprehensive cellular understanding of the cellular factors determining stress resistance.

Glucose metabolism is intimately tied to ATP production and is also required to generate metabolic intermediates for the synthesis of fatty acids, lipids, nucleotides, amino acids, and glycogen (Camandola and Mattson, 2017). As glucose metabolism is highly dependent on external factors such as oxygen, it must respond to cellular stresses such as hypoxia. Because the metabolic fate of glucose in cells depends on the selective expression of metabolic enzymes (Camandola and Mattson, 2017), adaptive responses may change the utilization of glucose by activating or inhibiting specific metabolic enzymes. Stresses such as hypoxic preconditioning trigger responses that increase the resistance of neurons to otherwise detrimental or even lethal conditions

(Gidday, 2006). However, little is presently known about potential maladaptive responses in neurons to hypoxia or other stresses.

In this study, we combined transcriptomic profiling with functional assays in primary mouse neurons and *Caenorhabditis elegans* animals to identify novel and conserved stress-responsive genes. We found that the metabolic enzyme *GDPGP1/mcp-1* is transcriptionally down-regulated in neurons across species, in response to a variety of stresses. Functional analysis indicates that *GDPGP1/mcp-1* is required to maintain normal stress resistance, potentially by controlling levels of neuronal glycogen. Animals without *GDPGP1/mcp-1* are sensitive to stress, while overexpressing *GDPGP1/mcp-1* in neurons confers stress resistance. Thus, down-regulation of *GDPGP1/mcp-1* is a maladaptive neuronal response, present from *C. elegans* to mouse, that limits the viability of neurons under stress.

Results

GDPGP1/mcp-1 is a novel stress-response gene

To identify a common transcriptional signature of neurons to acute stress, we used transcriptional profiling of cultured (7 days in vitro [DIV7]) primary mouse neurons under two different

¹Department of Genetics, Yale University, New Haven, CT; ²Department of Neuroscience, Yale University, New Haven, CT; ³Department of Neurology, Yale University, New Haven, CT; ⁴Leibniz Institute on Aging, Fritz Lipmann Institute, Jena, Germany.

Correspondence to Marc Hammarlund: marc.hammarlund@yale.edu; S.M. Han's present address is University of Florida, Gainesville, FL.

© 2019 Schulz et al. This article is distributed under the terms of an Attribution-Noncommercial-Share Alike-No Mirror Sites license for the first six months after the publication date (see <http://www.rupress.org/terms/>). After six months it is available under a Creative Commons License (Attribution-Noncommercial-Share Alike 4.0 International license, as described at <https://creativecommons.org/licenses/by-nc-sa/4.0/>).

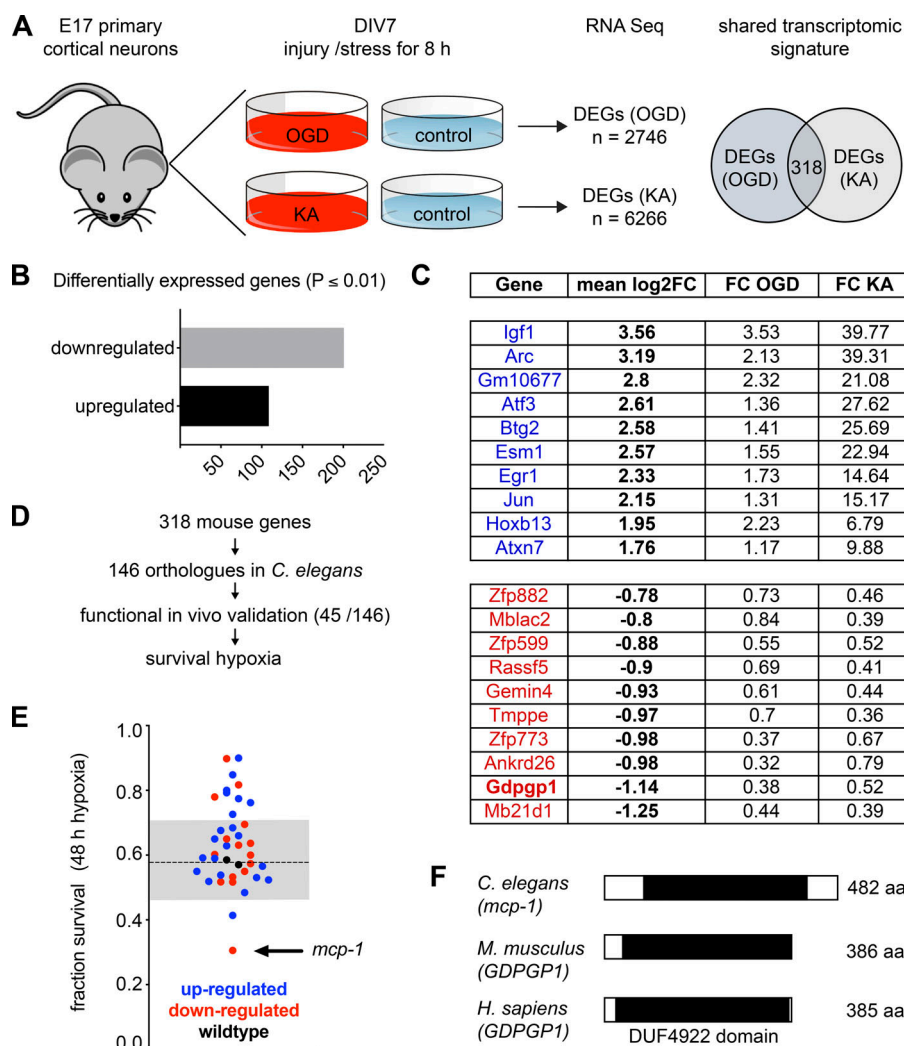


Figure 1. RNA-seq identifies the transcriptomic signature of acutely injured neurons. (A) Experimental design to generate a common transcriptomic signature of acutely injured primary mouse neurons. DIV7 neurons prepared from E17 mice were exposed to either OGD or KA. Differentially expressed genes (corrected P values ≤ 0.01) were determined for each condition. (B) Of 318 similarly regulated and statistically significant genes, 210 were found to be down-regulated and 108 up-regulated due to acute neuronal injury in both in vitro assays. (C) The top 10 up-regulated (blue) and down-regulated (red) genes identified as shared transcriptional signature of acutely injured neurons are depicted along with the mean log2 fold change (FC) and the individual FC for OGD and KA. (D) Flow chart illustrating the selection of identified genes for in vivo validation in *C. elegans*. (E) Graph indicating the results for 45 individual *C. elegans* mutant strains with regard to their survival during 48-h period of hypoxia. Each dot represents a single *C. elegans* strain tested. Mutant strains related to up-regulated genes are shown in blue, strains related to down-regulated genes in red. The dashed line depicts the performance of wild-type worms. The average SD calculated across all tested strains is depicted in gray. *mcp-1* mutant strain is highlighted by an arrow. (F) Comparison of GDPGP1/*mcp-1* protein domain and length (in aa) in *C. elegans*, mouse, and human. Each protein orthologue contains the same domain of unknown function (DUF4922).

stress conditions (Fig. 1 A). Oxygen-glucose deprivation (OGD) is a model for cerebral ischemia and has primary effects on cellular metabolism (Goldberg and Choi, 1993). Excitotoxicity, induced by the glutamate receptor agonist kainic acid (KA), is characterized by increased production of reactive oxygen species (ROS), mitochondrial dysfunction, and, eventually, neuronal apoptosis (Wang et al., 2005; Zheng et al., 2011). For each stressor, experimental conditions were used at which 20% of the cultured cells died due to an 8-h treatment (see Materials and methods). We identified differentially expressed genes in each condition. Next, the two conditions were compared, and 318 statistically significant transcripts were identified with similar regulation in the two different stress conditions (Fig. 1 B). Within these 318 genes, the known stress-responsive genes *Igf1*, *Arc*, *Atf3*, and *Jun* were among the 10 most up- and down-regulated genes (Fig. 1 C), suggesting that this approach successfully identifies stress-responsive genes.

Most of the 318 stress genes identified using this approach have no known functional role in stress. To discover which of these novel genes are functionally important with regard to stress in an in vivo model, we used the genetically tractable model *C. elegans*. Of 318 genes identified from primary mouse neurons, 146 were found to have *C. elegans* homologues (Shaye

and Greenwald, 2011; Fig. 1 D). We selected 45 genes for further testing based on the criteria of poor characterization, mutant availability, and nonlethality. 45 *C. elegans* strains, each bearing a single mutation in one of the selected genes, were analyzed for their survival under hypoxic conditions (Fig. 1 D). As 60% of wild-type animals survive a 48-h exposure to hypoxia (Fig. S1 A), our in vivo functional approach enabled the detection of survival rate changes in either direction. The hypoxia assay identified numerous mutants with altered survival after hypoxia (Fig. 1 E). We observed no correlation between whether genes were up- or down-regulated by stress in cultured mouse neurons and whether mutation of the gene conferred hypoxia resistance or sensitivity in *C. elegans*. Most mutants with an effect on hypoxia resistance, whether the orthologous genes were up- or down-regulated by stress in cultured mouse neurons, had increased resistance. However, one gene appeared particularly interesting in its function: its survival under hypoxia was the lowest of all tested strains (Fig. 1 E).

This mutant strain bears a loss-of-function mutation in the gene *mcp-1* (C10F3.4). Strikingly, its mammalian orthologue GDPGP1 (GDP-D-glucose phosphorylase 1) was one of the most down-regulated genes identified in the transcriptomic screen (Fig. 1 C). GDPGP1/*mcp-1* is evolutionarily conserved (Fig. 1 F) and

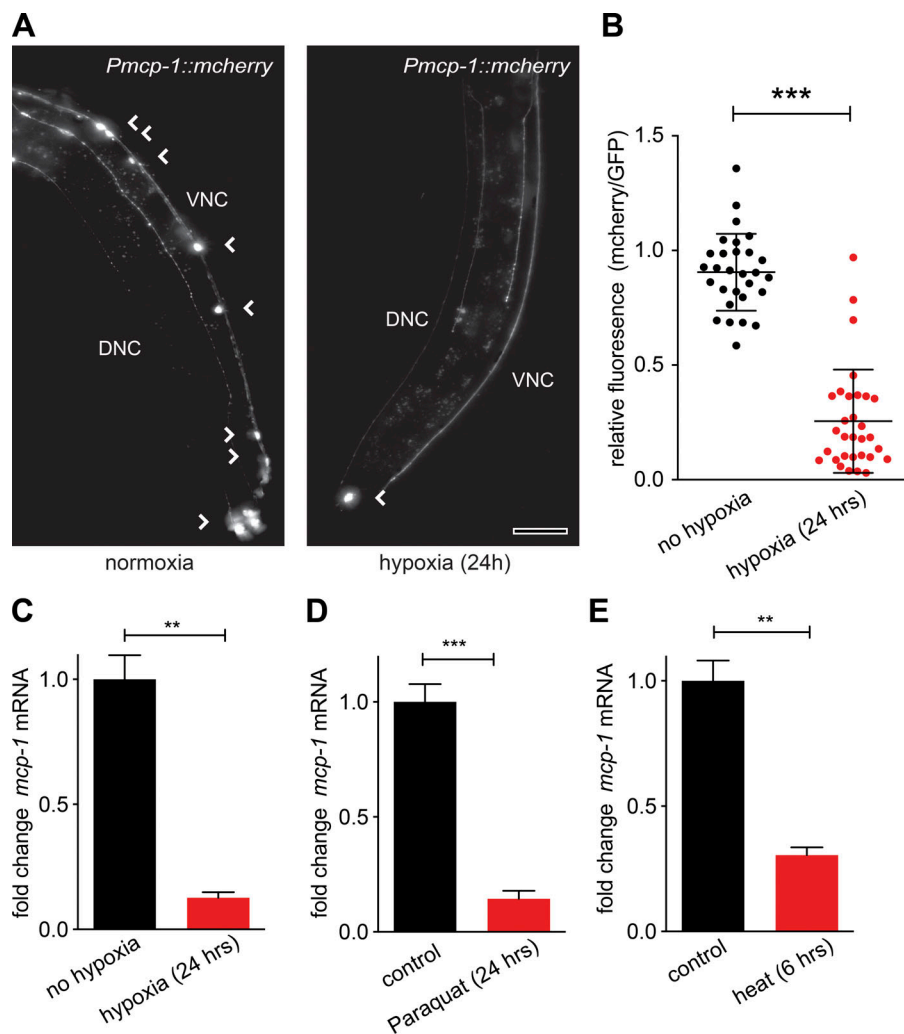


Figure 2. *mcp-1* is expressed in *C. elegans* neurons and is transcriptionally down-regulated during stress. (A) Fluorescent micrographs of animals expressing a transcriptional *mcp-1* reporter (*Pmcp-1::mCherry*). Left: Under normoxic conditions, expression is apparent in neuronal cell bodies (arrowheads), including neurons in the ventral nerve cord (VNC) and in the tail region. DNC, dorsal nerve cord. Right: Exposure to hypoxia (24 h) abolishes expression in cell bodies of most neurons. Scale bar, 50 μ m. (B) Quantification of relative fluorescence in *Pmcp-1::mCherry* animals relative to GFP (*Punc-25::GFP*; ***, $P < 0.001$; mean \pm SEM). (C–E) Quantitative RT-PCR analysis of *mcp-1* transcript levels in animals exposed to hypoxia (C), paraquat (D), and heat stress (E). All values were normalized to control treated animals and compared with actin expression levels (**, $P < 0.01$; ***, $P < 0.001$; mean \pm SEM).

was initially discovered in plants (the VTC2 gene) as part of the ascorbic acid synthesis machinery (Conklin et al., 2000). Although little of its physiological function and potential relevance in disease is currently known, a recent study in *C. elegans* found that *GDPGP1/mcp-1* functions in glucose metabolism by mediating the phosphorylation of GDP-glucose to glucose-1-phosphate (glucose-1-P; Adler et al., 2011). Given the strong in vivo phenotype of *GDPGP1/mcp-1* mutant animals, we focused on this gene for the remainder of this study.

In cultured mammalian neurons, *GDPGP1/mcp-1* expression is reduced by stress (Fig. 1 C). To determine whether a similar regulation occurs in *C. elegans*, we analyzed the expression of a transcriptional reporter for *mcp-1*, *Pmcp-1::mCherry*. Under basal conditions, we found that *Pmcp-1* drove mCherry expression predominantly in the nervous system (Fig. 2 A), consistent with previous results using a transcriptional reporter (Adler et al., 2011) and also consistent with single-cell transcriptional profiling (Cao et al., 2017). However, incubation under hypoxic conditions led to a drastic reduction of mCherry expression, to ~25% of normal levels (Fig. 2, A and B).

To confirm and extend this result, we performed additional stress assays and quantified endogenous *mcp-1* mRNA levels using quantitative PCR (qPCR) analysis. Incubation under hypoxic

conditions resulted in a marked decline of *mcp-1* transcript levels (Fig. 2 C). Exposure to ROS by paraquat treatment also decreased *mcp-1* mRNA levels (Fig. 2 D), as did heat stress (Fig. 2 E). Combined, these data indicate that *GDPGP1/mcp-1* is a stress-responsive gene with preferential expression in neuronal cells. In both mammalian and *C. elegans* neurons, *GDPGP1/mcp-1* expression is strongly down-regulated by multiple independent stresses. Further, the in vivo phenotype of *GDPGP1/mcp-1* *C. elegans* mutants suggests that *GDPGP1/mcp-1* regulation could have a key maladaptive role in the physiological response of neurons to cellular stress.

mcp-1 functions in neurons to combat multiple stresses

Mutant animals bearing the *mcp-1* loss-of-function allele *tm2679* (Adler et al., 2011) show normal development, anatomy (not depicted), and lifespan (Fig. 3 A). CRISPR/Cas9 was used to generate a second *mcp-1* loss-of-function allele (*wp38*), in which a frameshift mutation is introduced in the first exon, producing a truncated protein; like *tm2679* animals, these mutants appeared grossly wild type. However, consistent with results from *mcp-1(tm2679)* (Fig. 1 E), both alleles resulted in an ~50% decrease in survival rates after hypoxia (Fig. 3 B). To put this result in a wider context, we tested several *C. elegans* mutants related to the

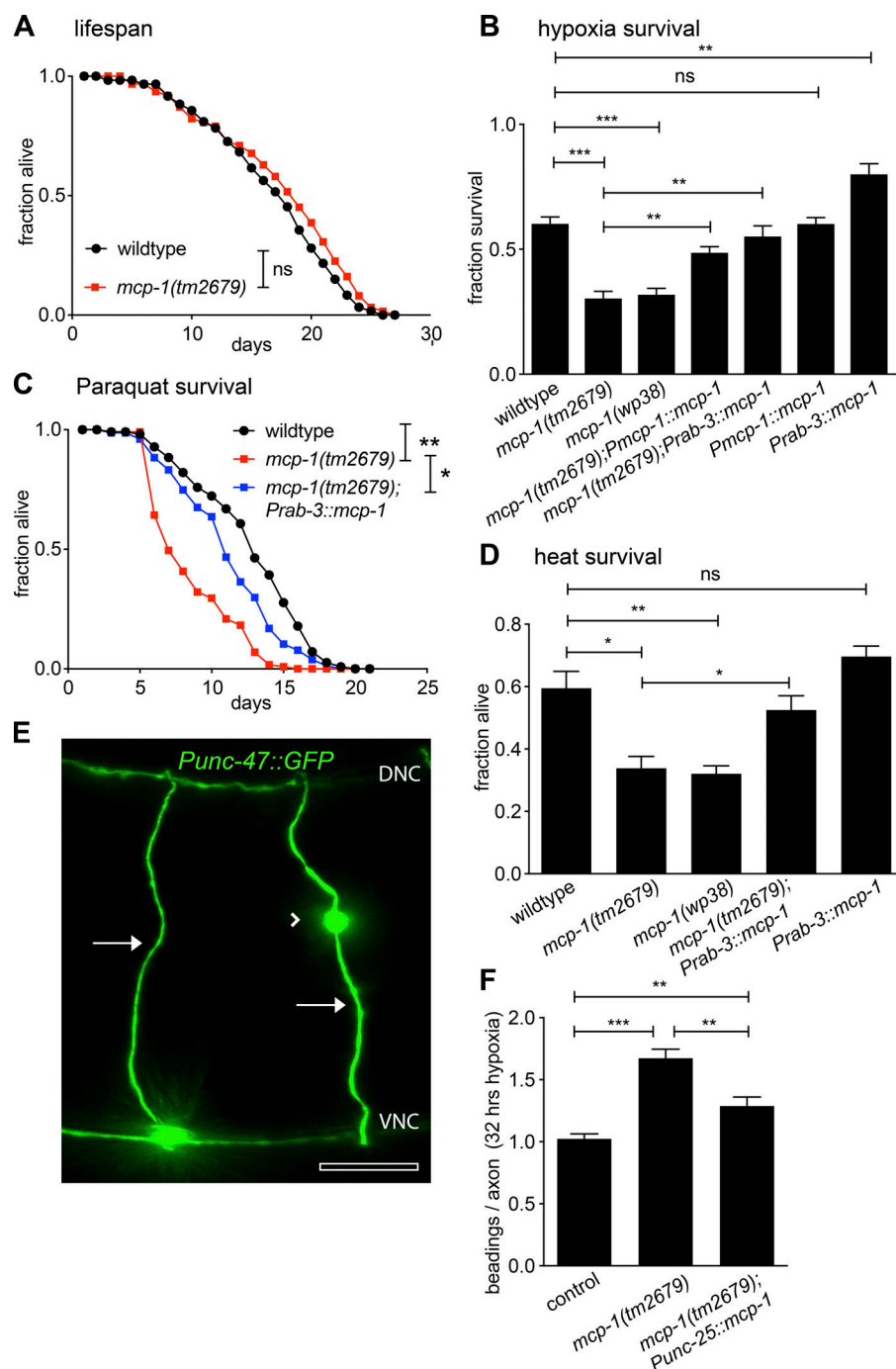


Figure 3. *mcp-1* functions in neurons to increase stress resistance. (A) Survival curves of wild-type and *mcp-1(tm2679)* mutant animals cultured on standard NGM plates at 25°C (ns, nonsignificant; log-rank test; $n > 100$ worms per genotype). (B) Survival of animals of indicated genotypes following 48-h exposure to hypoxia (*, $P < 0.01$; ***, $P < 0.001$; mean \pm SEM; $n > 100$ worms per genotype). (C) Survival curves of indicated genotypes on paraquat-treated NGM plates at 25°C (*, $P < 0.05$; **, $P < 0.01$; log-rank test; $n > 80$ per genotype). (D) Survival of L4 worms of indicated genotypes following exposure to a 6-h period of heat stress at 35°C (*, $P < 0.05$; **, $P < 0.01$; mean \pm SEM; $n > 100$ worms per genotype). (E) Representative fluorescent micrograph image of commissural axons (arrows) of GABA neurons visualized by *Punc-47::GFP* expression. A single axonal beading is indicated by arrowhead. Scale bar, 20 μ m. (F) Quantification of axonal beading per axon in indicated strains following 32 h of hypoxia (*, $P < 0.01$; ***, $P < 0.001$; mean \pm SEM; $n > 200$ axons per genotype).

hypoxia-inducible factor 1 (HIF-1) pathway, a master transcriptional regulator of adaptive responses to hypoxia (Majmundar et al., 2010). Although mutations in the HIF-1 pathway factor *egl-9* increased hypoxia survival, no HIF-1 pathway mutant resulted in decreased hypoxia survival, in contrast to mutations in *mcp-1* (Fig. S1 B).

Although *GDPGP1/mcp-1* expression in *C. elegans* was observed mainly in neurons (Fig. 2 A), *mcp-1* mutants exhibit decreased survival after hypoxia (Fig. 3 B), an organism-level response. To determine whether neuronal activity of *GDPGP1/mcp-1* is responsible for this organism-level response, neuron-specific rescue was performed. Reexpression of *mcp-1* under the pan-neuronal

promoter *Prab-3* was able to restore survival rates to wild-type levels, indicating that neuronal *mcp-1* function is sufficient for hypoxia resistance (Fig. 3 B). Neuron-specific expression also rescued the survival deficits of *mcp-1* mutants exposed to paraquat (Fig. 3 C) and to heat stress (Fig. 3 D). Interestingly, tissue-specific reexpression of *mcp-1* in nonneuronal tissues (body wall muscles and the hypodermis, using the *myo-3*, *col-19*, and *dpy-7* promoters, respectively) also rescued the survival deficits of *mcp-1* mutants under hypoxia (Fig. S1 C). Thus, expression of *GDPGP1/mcp-1* in neurons is sufficient for its function in stress resistance, and expression outside of the normal neuronal context can compensate for loss of this neuronal function.

GDPGP1/mcp-1 mutants have poor stress resistance (Fig. 3, B–D), and *GDPGP1/mcp-1* transcription is down-regulated by stress (Fig. 2, A–E). These data suggest that, in wild-type animals, down-regulation of *GDPGP1/mcp-1* in neurons may be a maladaptive response to stress that results in decreased survival. This was tested by overexpressing *mcp-1* in wild-type animals under the *rab-3* promoter, which is neuron specific and unlikely to be stress responsive. We found that neuronal overexpression of *GDPGP1/mcp-1* enhanced survival after hypoxia to ~80% above wild-type levels (Fig. 3 B, compare wild type to *Prab-3::mcp-1*). Tissue-specific overexpression of *mcp-1* in nonneuronal body wall muscles or hypodermis also enhanced survival above wild-type levels (Fig. S1 D). Thus, expression of *mcp-1* is a critical determinant of hypoxia resistance in *C. elegans*, with increased expression conferring increased survival.

Neuronal *mcp-1* regulates organism-level survival, suggesting that it may also act cell-intrinsically to protect neurons. This idea was tested by examining the consequences of *mcp-1* loss of function on a cellular level in neurons. Axonal beadings (Fig. 3 E) are a common feature of neurodegenerative diseases and frequently precede cell body death (Beirowski et al., 2010; Coleman, 2005). Previous studies found that axonal beadings can be provoked in *C. elegans* by exposure to sublethal hypoxia (Scott et al., 2002). Consistent with these results, we observed that beadings increased with hypoxia duration and that 32 h of hypoxia resulted in an average of one beading per axon (Fig. S1 E). Under these conditions, we found that axons of γ -aminobutyric acid (GABA) neurons in *mcp-1* knockout worms showed a marked increase in the number of beadings per axon compared with wild-type animals (Fig. 3 F). Occasionally, the breakage and fragmentation of axons in *mcp-1* mutant worms under hypoxia was detected (Fig. S1 F), a phenomenon not observed in control animals. Re-expression of *mcp-1* only in GABA neurons (*mcp-1(tm2679);Punc-25::mcp-1*) was sufficient to rescue the effect of loss of *mcp-1*, indicating that *GDPGP1/mcp-1* functions cell autonomously in neurons to limit the effects of hypoxia (Fig. 3 F). Overall, our data indicate that neuronal *GDPGP1/mcp-1* plays a key, cell-intrinsic role in neuronal responses to a wide variety of stresses and injuries.

GDPGP1 knockdown in primary mouse neurons results in neurodegeneration

Like *C. elegans mcp-1*, expression of *GDPGP1* in cultured primary mouse neurons is transcriptionally down-regulated in response to stress (Fig. 1 C). These RNA-sequencing (RNA-seq) results were confirmed and extended by quantifying *GDPGP1* transcript levels under various stress conditions using qPCR. Both OGD (Fig. 4 A) and exposure to the ROS-generating compound paraquat (Fig. 4 B) resulted in loss of most *GDPGP1* mRNA expression. To confirm that this decrease in mRNA was relevant for protein expression, we performed Western blotting of primary cells following exposure to the same stress conditions. Consistent with the mRNA results, we found that *GDPGP1* protein in mouse neurons (Fig. S2 A for expression) was down-regulated by stress (Fig. 4 C). Thus, the down-regulation of *GDPGP1/mcp-1* in response to stress is conserved across species in neurons.

Next, we tested whether *GDPGP1/mcp-1* has a neuroprotective functional role in mouse neurons similar to that in *C. elegans*. An

shRNA-mediated knockdown of *GDPGP1* (*shGDPGP1*) in primary neurons reduced *GDPGP1* protein levels (Fig. S2 B). This treatment had no obvious effect on the morphology or survival rate of neurons 3 d after transfection (Fig. 4 D). However, while control transfected neurons showed elaborate neurite branching 7 d after transfection, *GDPGP1* knockdown cells were mostly apparent as shrunken cell remnants (Fig. 4 D). Quantification of viable cells revealed a steady degeneration of primary neurons following *GDPGP1* knockdown beginning 4 d after transfection (Fig. 4 E). Coexpression of the human *GDPGP1* coding sequence (*hGDPGP1*), along with the knockdown construct, could partially rescue this widespread neurodegeneration, indicating that this phenotype is specific to knockdown of *GDPGP1* (Fig. 4 E). Furthermore, administration of the pan-caspase inhibitor Z-VAD-FMK to the culture medium following the transfection of cells also resulted in decreased neurodegeneration (Fig. 4 E), indicating that *GDPGP1* knockdown promotes apoptotic cell death in primary mouse neurons.

Next, we investigated the nature of the neuronal response to *shGDPGP1* at 4 d after transfection, when neurodegeneration in *GDPGP1*-deficient neurons is still limited. It was found that increased activation of Caspase-3 could be detected after shRNA-mediated knockdown compared with control transfected neurons (Fig. 4 F). Cleaved Caspase-3 levels could be rescued by coexpressing *hGDPGP1* and by applying the pan-caspase inhibitor Z-VAD-FMK to the culture medium, further suggesting that *GDPGP1* knockdown promotes apoptotic cell death.

In addition, we found that a number of other stress-related proteins were up-regulated in response to shRNA-mediated *GDPGP1* knockdown in neurons, including Dkk-4, Hsp60, and SIRT2 (Fig. S2, C–E). Thus, loss of *GDPGP1/mcp-1* affects neurons in both *C. elegans* and cultured mouse neurons, but the effect is stronger in vitro. In *C. elegans*, loss of *GDPGP1/mcp-1* causes an overt phenotype only in response to stress, while in cultured mouse neurons, loss of *GDPGP1/mcp-1* is cell-lethal even under standard culture conditions.

GDPGP1/mcp-1 regulates neuronal glycogen levels

GDPGP1/mcp-1 is a phosphorylase that catalyzes the conversion of GDP-glucose to glucose-1-phosphate and GDP (Fig. 5 A); and *mcp-1* loss-of-function worms accumulate GDP-glucose (Adler et al., 2011). To understand how *GDPGP1/mcp-1* contributes to neuronal stress resistance, we sought to determine whether other metabolites and cellular processes linked to glucose-1-P production are affected by loss of *GDPGP1/mcp-1*. Consistent with *GDPGP1/mcp-1*'s enzymatic function, we found that glucose-1-P levels were significantly decreased in both *mcp-1*-deficient worms (Fig. 5 B) and in primary culture mouse neurons following *GDPGP1* knockdown (Fig. 5 C). (Experiments in primary culture mouse neurons were performed at DIV4, a time point at which cell death is similar to controls; Fig. 4 E). In contrast, glucose-6-P and pyruvate levels were not affected (Fig. S3, A–D). Further, genetic inhibition of glycolysis by mutating its rate-limiting enzyme *pfk-1.1* did not affect *C. elegans* survival under hypoxia, unlike the loss of *mcp-1* (Fig. S3 E). Thus, loss of *GDPGP1/mcp-1* specifically affects steady-state levels of glucose-1-P, but not glucose-6-P or pyruvate.

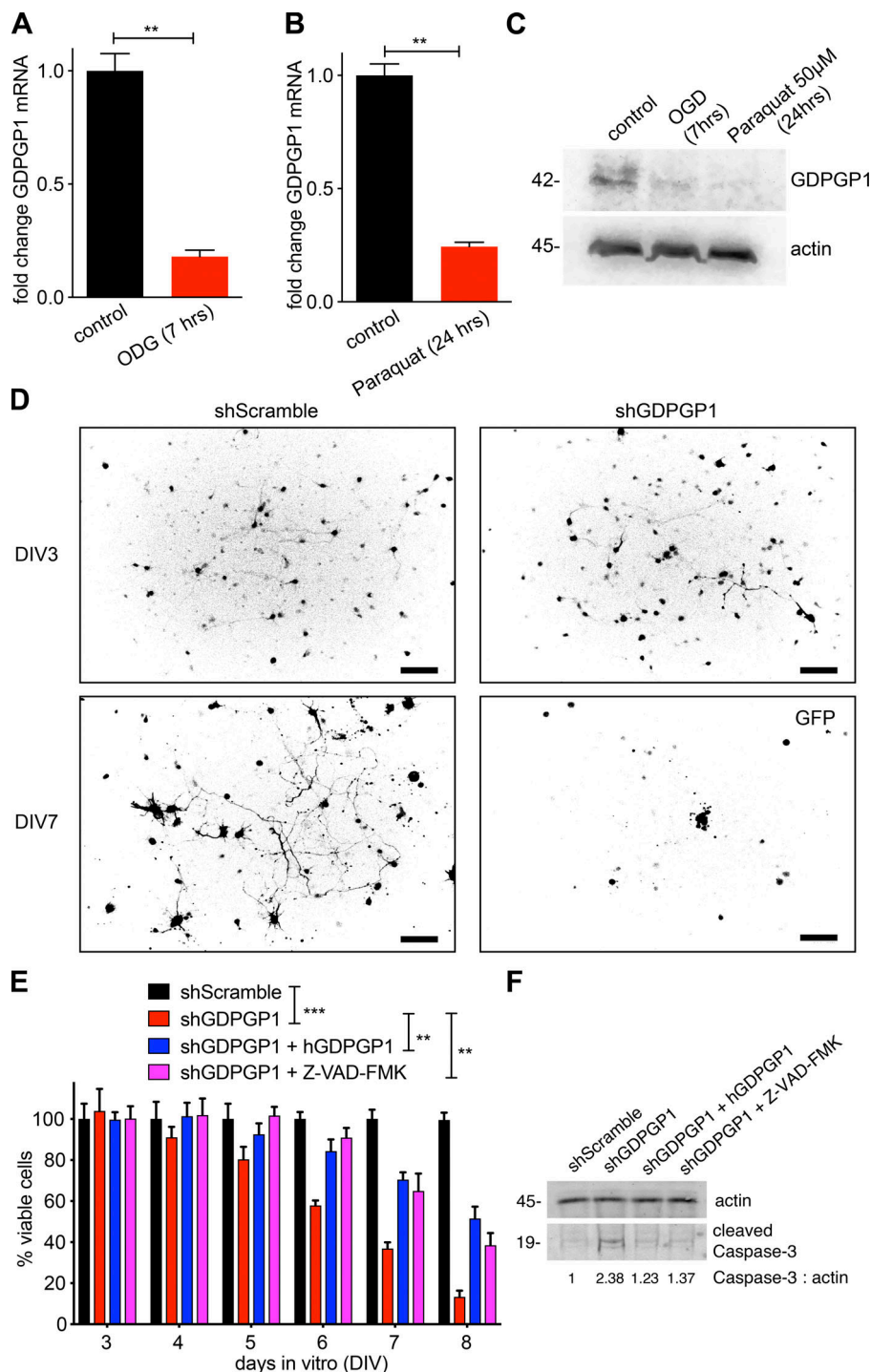


Figure 4. GDPGP1 is down-regulated by stress, and its knockdown leads to neuro-degeneration in mouse neurons. (A and B) Quantitative RT-PCR analysis of *GDPGP1* transcript levels in DIV7 primary mouse neurons exposed to OGD (A) and paraquat (B). All values were normalized to control treated neurons and compared with actin expression levels (**, $P < 0.01$; mean \pm SEM; $n = 3$). **(C)** Immunoblot of cell lysates prepared from DIV7 primary mouse neurons after exposure to OGD and paraquat for GDPGP1 and actin as loading control ($n = 3$). **(D)** Representative fluorescent micrographs of cultured primary neurons transfected with either scrambled (shScramble) or GDPGP1-targeted (shGDPGP1) shRNA constructs at two different time points (DIV3 and DIV7). Only transfected, GFP-positive neurons are visualized (GFP is coexpressed in pAAV-U6-GFP vector). Scale bar, 50 μ m. **(E)** Quantification of viable cells in cultures of primary neurons over time (DIV3 to DIV8). Neurons were transfected at DIV0 with scrambled control (shScramble), GDPGP1-targeted (shGDPGP1) shRNA constructs, GDPGP1-targeted shRNA constructs plus the *hGDPGP1* coding sequence (shGDPGP1 + *hGDPGP1*), or GDPGP1-targeted shRNA constructs plus the pan-caspase inhibitor Z-VAD-FMK (shGDPGP1 + Z-VAD-FMK). All values were normalized to control transfected neurons (shScramble) at each time point (**, $P < 0.01$; ***, $P < 0.001$; two-way ANOVA for repeated measures with Holm-Sidak post hoc test; $n > 250$ neurons per genotype and time point; mean \pm SEM). **(F)** Immunoblot of cell lysates prepared from DIV4 primary mouse neurons transfected with either scrambled (shScramble), GDPGP1-targeted (shGDPGP1) shRNA constructs, GDPGP1-targeted shRNA constructs plus the *hGDPGP1* coding sequence (shGDPGP1 + *hGDPGP1*), or GDPGP1-targeted shRNA constructs plus the pan-caspase inhibitor Z-VAD-FMK (shGDPGP1 + Z-VAD-FMK) for cleaved Caspase-3 and actin as loading control. Densitometric quantification of Caspase-3/actin ratio was normalized to shScramble ($n = 3$).

Besides conversion to glucose-6-P, glucose-1-P can also be converted to glycogen, which is essentially a storage depot for glucose-1-P (Fig. 5 A). Although present mainly in liver and muscle tissue, glycogen is also the single largest energy reserve in the brain (Falkowska et al., 2015). Further, genetic inhibition of glycogen synthesis has been shown to reduce the survival rate of *C. elegans* under hypoxic conditions (LaMacchia et al., 2015). However, glycogen is thought to be present mainly in glia, rather than neurons (Waite et al., 2017). To examine the potential link between *GDPGP1*/*mcp-1* and glycogen, glycogen levels were measured. In *C. elegans*,

glycogen levels were reduced in *mcp-1* mutant animals, and this deficit was rescued by neuron-specific reexpression of *mcp-1* (Fig. 5 D). Tissue-specific reexpression of *mcp-1* in nonneuronal cells such as body wall muscles, the gut, and the hypodermis, on the other hand, was not sufficient to rescue the observed drop in glycogen levels in *mcp-1* mutant animals (Fig. S3 F). Thus, in *C. elegans*, neuronal *mcp-1* maintains glycogen levels (Fig. 5 D and Fig. S3 F) and enhances the ability of animals to survive hypoxia (Fig. 3 B and Fig. S1, C and D), suggesting that neuronal *mcp-1* function in glycogen metabolism is critical for hypoxia survival.

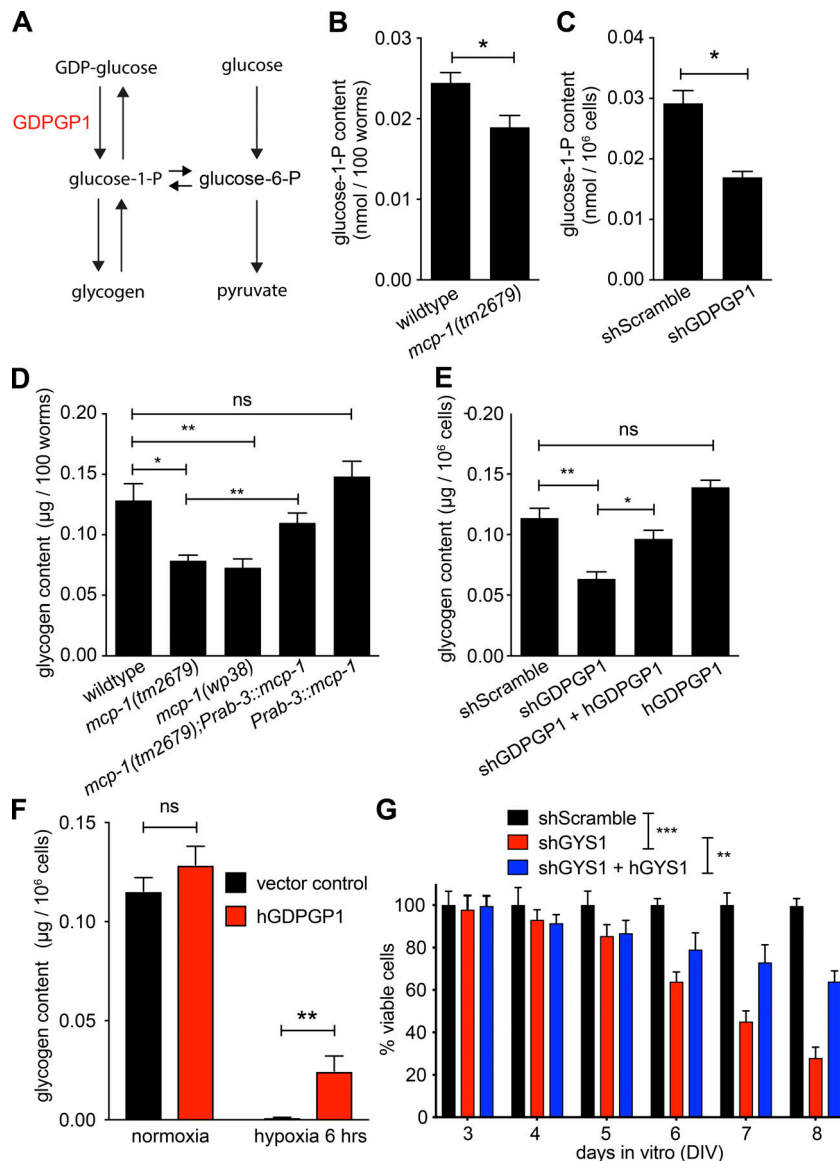


Figure 5. Loss of *mcp-1/GDPGP1* decreases neuronal glycogen levels. (A) Overview of reactions in glucose metabolism involving glucose-1-P and related metabolites. (B) Quantification of glucose-1-P levels in L4 nematodes of indicated genotypes (*, $P < 0.05$; mean \pm SEM; $n = 4$). (C) Quantification of glucose-1-P levels in cell lysates prepared from DIV4 primary mouse neurons transfected with scrambled control (shScramble) and GDPGP1-targeted (shGDPGP1) shRNA constructs (*, $P < 0.05$; mean \pm SEM; $n = 3$). (D) Quantification of glycogen content in L4 nematodes of indicated genotypes (*, $P < 0.05$; **, $P < 0.01$; ns, nonsignificant; mean \pm SEM; $n = 4$). (E) Quantification of glycogen content in cell lysates prepared from DIV4 primary mouse neurons transfected with shScramble, GDPGP1-targeted (shGDPGP1) shRNA constructs, or GDPGP1-targeted shRNA constructs plus the hGDPGP1 coding sequence (shGDPGP1 + hGDPGP1; *, $P < 0.05$; **, $P < 0.01$; mean \pm SEM; $n = 3$). (F) Quantification of glycogen content in cell lysates prepared from DIV4 primary mouse neurons transfected with vector control or the hGDPGP1 coding sequence (hGDPGP1). Neurons were kept at either standard culture conditions (normoxia) or 6-h hypoxia before lysate preparation (**, $P < 0.05$; mean \pm SEM; $n = 3$). (G) Quantification of viable cells in cultures of primary neurons over time (DIV3 to DIV8). Neurons were transfected at DIV0 with shScramble, GYS1-targeted (shGYS1) shRNA constructs, or GYS1-targeted shRNA constructs plus the hGYS1 coding sequence (shGYS1 + hGYS1). All values were normalized to control transfected neurons (shScramble) at each time point (**, $P < 0.01$; ***, $P < 0.001$; two-way ANOVA for repeated measures with Holm-Sidak post hoc test; $n > 150$ neurons per genotype and time point; mean \pm SEM).

In primary mouse neurons, shRNA-mediated GDPGP1 knockdown also reduced glycogen content, consistent with our observations in *C. elegans* (Fig. 5 E). Cotransfection of hGDPGP1 along with the knockdown construct could partially rescue this effect. Together, these data indicate that a reduction in glycogen levels is a primary result of loss of GDPGP1/*mcp-1* in neurons across species. Next, we tested whether decreased glycogen levels could account for the reduced resistance to hypoxia observed due to loss of GDPGP1/*mcp-1* in cultured neurons. Exposure of primary neurons to a 6-h period of hypoxia caused the total depletion of internal glycogen stores (Fig. 5 F). In contrast, neurons overexpressing GDPGP1/*mcp-1* (by transfection with hGDPGP1) were capable of preserving some glycogen after the same exposure to hypoxic culture conditions (Fig. 5 F). Together, these data indicate that GDPGP1 acts in neurons to maintain neuronal glycogen stores.

To directly test the function of glycogen in neuronal survival, we performed knockdown of the glycogen-producing enzyme glycogen synthase (GYS1) in primary neurons. GYS1 knockdown phenocopied the knockdown of GDPGP1, resulting in widespread

neuronal death with a similar magnitude and time course (Fig. 5 G, compare with Fig. 4 E). Coexpression of the hGYS1 coding sequence, along with the knockdown construct, could partially rescue this widespread neurodegeneration, indicating that this phenotype is specific to knockdown of GYS1 (Fig. 5 G). Similarly, genetic inhibition of the glycogen-degrading enzyme in *C. elegans*, glycogen phosphorylase (*pygl-1*), which is predominantly expressed in neuronal cells and body wall muscle tissue (Cao et al., 2017), leads to improved survival of worms under hypoxia (Fig. S3 G), similar to the effect of overexpression of *mcp-1* (Fig. 3 B). Overall, these data suggest that GDPGP1/*mcp-1* affects the stress resistance of neurons by regulating internal glycogen levels and that glycogen levels affect the stress resistance of neurons.

Increased *mcp-1* ameliorates the phenotype of a tauopathy model

Hypoxia is a relatively acute stress; by contrast, many neurodegenerative diseases operate on a longer time scale. To test the

ability of *mcp-1* to protect neurons from more chronic stresses, we examined the effect of *GDPGPI/mcp-1* in a *C. elegans* model of tauopathy. The nematode strain Paex-3::htauV337M expresses the htau gene (*MAPT*) carrying the V337M mutation in the nervous system under the *aex-3* promoter (Guthrie et al., 2009). Analogous to frontotemporal dementia with parkinsonism chromosome 17 type, Paex-3::htauV337M animals display an uncoordinated behavioral phenotype that progressively worsens with age (Kraemer et al., 2003). At the cellular level, degeneration can be assessed as multiple axonal discontinuities in the GABAergic nervous system (Fig. 6 A). We found that, compared with wild-type worms, Paex-3::htauV337M animals have reduced *mcp-1* transcript levels (Fig. 6 B), suggesting that stress in this model, most probably intracellular aggregation of tau filaments in neurons (Nacharaju et al., 1999), is another kind of stress that provokes *mcp-1* down-regulation. Worms expressing wild-type (non-V337M) htau in the nervous system, Paex-3::htau (Taylor et al., 2018), also displayed lower *mcp-1* transcript levels, but not to the extent of Paex-3::htauV337M worms. We conclude that even overexpression of wild-type tau can partially stress neurons and down-regulate *mcp-1*, but that overexpression of mutant tau has a stronger effect.

To determine the potential function of *mcp-1* in the tauopathy model, we first examined glycogen levels. We found that Paex-3::htauV337M animals have reduced levels of glycogen (Fig. 6 C), consistent with the idea that reduced *mcp-1* levels cause a depletion of neuronal glycogen stores (Fig. 5 D). Thus, like acute stresses such as hypoxia, ROS, and heat (Fig. 2, C–E), the Paex-3::htauV337M tauopathy model results in down-regulation of *GDPGPI/mcp-1* and is associated with reduced glycogen.

Overexpression of *GDPGPI/mcp-1* in neurons protects *C. elegans* from hypoxia and increases glycogen in cultured mouse neurons following acute hypoxic stress (Figs. 3 B and 5 F). We tested the ability of neuronal *GDPGPI/mcp-1* to ameliorate the neurodegenerative phenotype of the tauopathy model by overexpressing *GDPGPI/mcp-1* in the Paex-3::htauV337M background exclusively in neuronal cells (using the *rab-3* promoter). Paex-3::htauV337M animals display abnormal movement, which is clearly evident from their inability to leave a regular sinusoidal track in the bacterial lawn (Fig. 6 D). We found that pan-neuronal expression of *mcp-1* (Paex-3::htauV337M;*Prab-3::mcp-1*) improved the performance of Paex-3::htauV337M in this assay (Fig. 6 D). To confirm and extend these results, a thrashing assay was used as an alternative functional measure. Compared with wild-type animals, Paex-3::htauV337M worms showed a marked reduction in thrashing behavior, consistent with neuronal defects (Fig. 6 E). Knockout of *mcp-1* in Paex-3::htauV337M worms (Paex-3::htauV337M;*mcp-1(tm2679)*) did not aggravate the phenotype of Paex-3::htauV337M worms (Fig. 6 E). However, pan-neuronal overexpression of *mcp-1* (Paex-3::htauV337M;*Prab-3::mcp-1*) improved the uncoordinated movement in Paex-3::htauV337M worms (Fig. 6 E).

In addition to these behavioral measures, we tested the ability of *GDPGPI/mcp-1* overexpression to suppress the cellular abnormalities found in GABA neurons of Paex-3::htauV337M animals (Fig. 6 A). We found that overexpression of *mcp-1* either in all neurons (Paex-3::htauV337M;*Prab-3::mcp-1*) or in only

GABA neurons reduced the number of axonal discontinuities in GABA neurons in the Paex-3::htauV337M background (Fig. 6 F), indicating that *mcp-1* acts cell intrinsically to resist degeneration. However, unlike pan-neuronal expression, GABA neuron-specific expression of *mcp-1* in Paex-3::htauV337M worms (Paex-3::htauV337M;*Punc-25::mcp-1*) had no effect on the overall movement phenotype (Fig. 6 D) and did not improve thrashing performance (Fig. 6 E), indicating that the effects of *mcp-1* expression are limited to the cells in which it is expressed. Together, these data indicate that neuronal *GDPGPI/mcp-1* expression can protect neurons against the chronic stress of a tauopathy model at both morphological and functional levels.

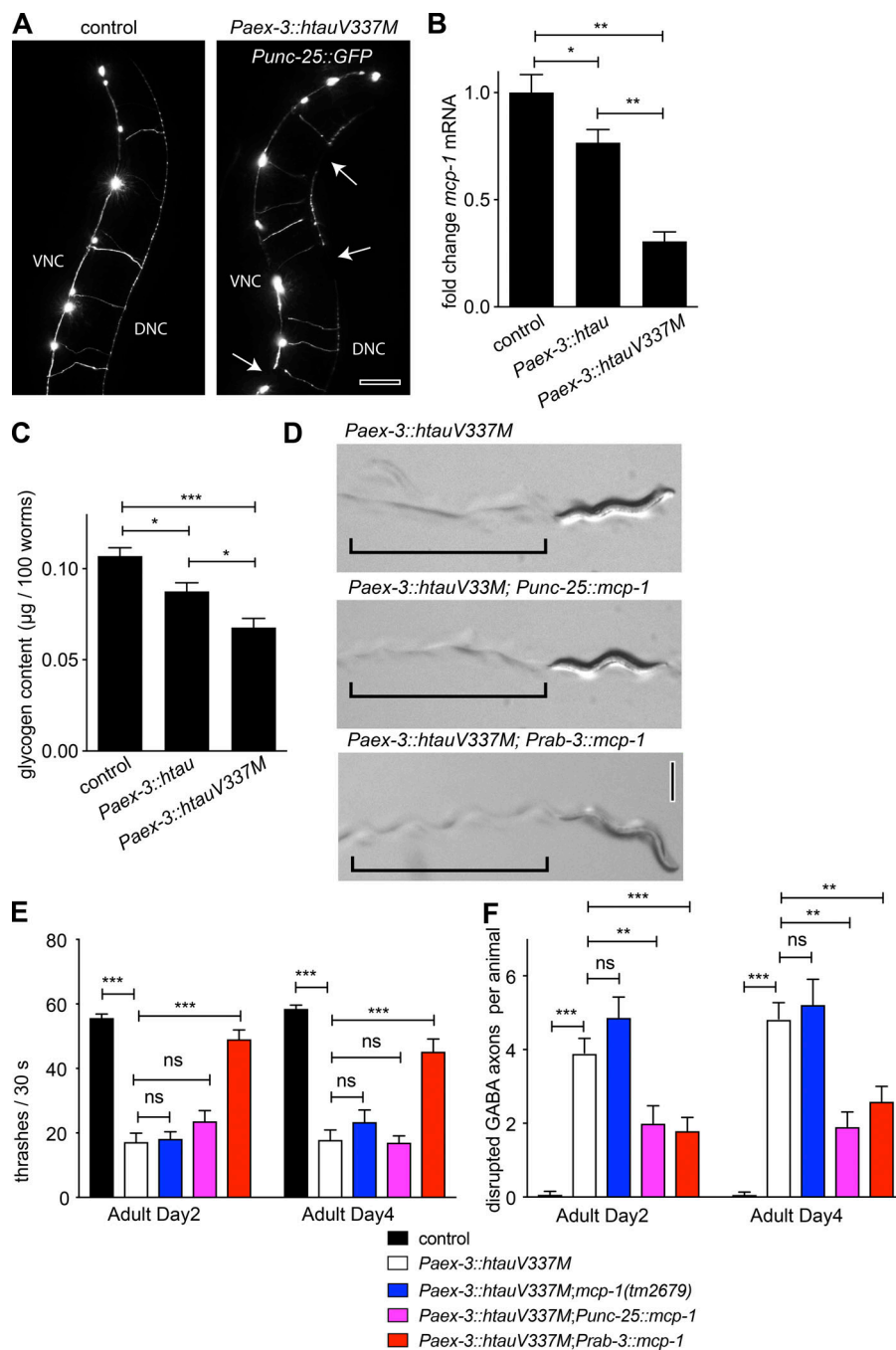
Discussion

We identified the *C. elegans* gene *mcp-1* and its mammalian homologue *GDPGPI* as a novel mechanism, conserved across phyla, by which neurons respond to both intrinsic and environment-induced stress (Fig. 7). *GDPGPI/mcp-1* expression in neurons is required for normal resistance to a wide variety of stresses, and overexpression of *GDPGPI/mcp-1* increases resistance to both acute and chronic stresses. Thus, *GDPGPI/mcp-1* is a potent neuroprotective molecule.

In *C. elegans*, loss of *GDPGPI/mcp-1* results in decreased survival and enhanced axon degeneration under hypoxic conditions. By contrast, in primary mouse neurons, the knockdown of *GDPGPI* provokes widespread neuronal death, even in the absence of additional environmental stress factors. One possible explanation for this differential reliance on *GDPGPI/mcp-1* is that cultured embryonic cortical neurons are more dependent on glycolysis. Consistent with this idea, various studies have reported metabolic changes over the course of neuronal development (Agostini et al., 2016; Zheng et al., 2016). It is also possible that the nature of the gene reduction contributes to the difference in phenotype, with *C. elegans* neurons better able to compensate for loss of *GDPGPI/mcp-1* function due to the chronic nature of the genetic loss-of-function mutation (De Souza et al., 2006; Williams et al., 2015).

Despite these differences, the regulation and function of *GDPGPI/mcp-1* in neuronal stress is remarkably well conserved between these two different models. In both *C. elegans* and mouse culture systems, multiple stresses result in the transcriptional down-regulation of *GDPGPI/mcp-1*. Neurons in both systems with less *GDPGPI/mcp-1* are more sensitive to a variety of stresses, while overexpression of *GDPGPI/mcp-1* renders neurons more resistant to stress. Further, despite its position at a key node of glucose metabolism (Fig. 5 A), *GDPGPI/mcp-1* is not expressed in all tissues. In *C. elegans*, *GDPGPI/mcp-1* is expressed primarily in neurons (Fig. 2 A; Adler et al., 2011; Cao et al., 2017). Data from the Human Protein Atlas indicate that, in vertebrates, *GDPGPI* has highest expression in brain tissue as well as in a few glycogen-rich organs such as muscle and liver (Uhlén et al., 2015). Thus, neurons seem to have a specialized mechanism for controlling glucose metabolism that is intimately associated with their ability to withstand stress.

In a variety of assays in both *C. elegans* and cultured mouse neurons, *GDPGPI/mcp-1* is transcriptionally down-regulated by



stress. The fact that this regulatory function is present across species suggests that *GDPGP1/mcp-1* regulation under stress is a conserved and ancient feature of nervous systems. Overall, our data indicate that *GDPGP1/mcp-1* transcriptional down-regulation is a maladaptive response to stress. However, it is possible that down-regulation of *GDPGP1* might be protective under some stress conditions not identified in this study. Identifying and understanding such maladaptive responses and their regulation may indicate unexpected possibilities for helping neurons better survive stress.

Our data suggest that glycogen may be a key metabolite that affects neuronal stress resistance in concert with *GDPGP1/mcp-1*. Along with glucose-1-P, the direct end product of *GDPGP1/mcp-1*

activity, we found that *GDPGP1/mcp-1* affects cellular levels of glycogen in both *C. elegans* and cultured neurons. Loss of *GDPGP1/mcp-1* reduced glycogen, as did hypoxia. Overexpression of *GDPGP1/mcp-1* increased glycogen under hypoxia. Further, knockdown of glycogen synthase phenocopied the loss of *GDPGP1/mcp-1* in cultured neurons. Consistent with these results, loss of glycogen synthase has been found to cause hypoxia sensitivity in cultured neurons (Saez et al., 2014). Thus, our data support the emerging idea that glycogen plays a critical role in neurons.

Glycogen is synthesized from UDP-glucose, and UDP-glucose is synthesized from glucose-1-P. A major source of glucose-1-P is from conversion of glucose-6-P by phosphoglucosmutase.

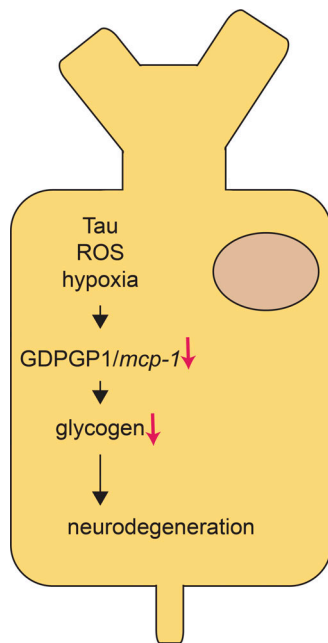


Figure 7. **Proposed model of GDPGP1/mcp-1's function in neuronal stress response.** Upon injury or damage to neuronal cells, a response program is initiated that involves down-regulation of GDPGP1/mcp-1 transcript and protein levels. GDPGP1/mcp-1 down-regulation results in lower glucose-1-P levels and lower neuronal glycogen content. Reduction of these metabolites causes neurodegeneration and decreases the stress resistance of neurons.

However, phosphoglucomutase also catalyzes the reverse reaction (from glucose-1-P to glucose-6-P), and thus may not drive maximum glucose-1-P levels and glycogen accumulation. Further, phosphoglucomutase is expressed at low levels in *C. elegans* neurons relative to other tissues (Cao et al., 2017). By contrast, GDPGP1/mcp-1 is robustly expressed in *C. elegans* neurons and provides a different source of glucose-1-P, from conversion of GDP-glucose. Thus, expression of GDPGP1/mcp-1 may drive glycogen accumulation, both in its normal context in neurons and when misexpressed in other tissues, by providing elevated levels of glucose-1-P. Although GDPGP1/mcp-1 misexpression did result in hypoxia resistance (Fig. S1), misexpression did not have a detectable effect on glycogen levels in our assay conditions, in contrast to the effect of expression in neurons (Fig. S3), possibly because mis-expressed GDPGP1/mcp-1 is not fully active under our assay conditions. Overall, our data indicate that GDPGP1/mcp-1 is an essential enzyme for glucose-1-P production, and that glucose-1-P in neurons is a critical determinant of neuronal glycogen levels and ability to withstand hypoxia.

Materials and methods

Primary neuron culture

Primary cortical cultures were established from E17 C57BL/6 mice. Cortices were dissected in ice-cold Hibernate E medium (HE-Ca; BrainBits) and incubated in HBSS digestion medium containing 30 U/ml Papain (LS003127; Worthington Biochemical), 1.5 mM CaCl₂, 2.5 mM EDTA, and 2 mg/ml DNaseI (DN25; Sigma-Aldrich) at 37°C for 20 min. Digested tissues were triturated and suspended in Neurobasal-A. Cells were plated on 6-well tissue

culture plates coated with poly-D-lysine at a density of 5×10^5 cells per well in 2.5 ml of Neurobasal-A medium, supplemented with B-27, GlutaMAX, and penicillin-streptomycin (all from Invitrogen). The pan-caspase inhibitor Z-VAD-FMK (60332, Cell Signaling) was added to the culture medium to block apoptosis at a concentration of 10 μ M.

In vitro injury assays of primary neurons

Primary cortical forebrain neurons were prepared from E17 animals. Arabinofuranosyl cytidine (working concentration 10 mM, Sigma-Aldrich) was used in the first 7 d to ensure glia-free conditions of the cultures. After 7 DIV, neuronal cultures were treated with either KA (100 μ M in culture medium; K0250; Sigma-Aldrich) or OGD for 8 h. OGD was achieved by culturing cells in Neurobasal medium without glucose (0050128DJ; Life Technologies) in a hypoxic incubator, under the following conditions: 1% O₂, 5% CO₂, saturated humidity atmosphere, and 37°C. Control cells were treated with PBS (KA) and Neurobasal medium with glucose, at regular incubator conditions (OGD). The conditions for the assays were determined in preliminary experiments to achieve a cell death rate of 20% after 8-h treatments. Cell death was analyzed by Trypan blue staining.

RNA-seq

Total RNA was extracted using RNeasy Mini Kit (Qiagen). RNA samples were sequenced using Illumina's next-generation sequencing methodology (Bentley et al., 2008). Briefly, quality check and quantification of total RNA were performed using the Agilent Bioanalyzer 2100 in combination with the RNA 6000 nano kit (Agilent Technologies). Illumina's TruSeq RNA v.2 library preparation kit was used for library preparation, according to manufacturer's instructions. Quantification and quality check of libraries were completed using the Agilent Bioanalyzer 2100 in combination with the DNA 7500 kit. Libraries were sequenced on a HiSeq2500 running in 51 cycle/single-end/rapid mode. All libraries were pooled and sequenced in two lanes. Sequence information was extracted in FastQ format using Illumina's bcl2fastq v.1.8.4. Sequencing resulted in an average of ~33 million reads per sample.

RNA-seq data analysis

Reads were mapped to the mouse reference mm10, taking the refSeq annotation (v.2014-04-25) into account, using Tophat v.1.4.1 (Trapnell et al., 2009; parameter: -T -x 1-no-novel-juncs). Reference genome and annotation were downloaded from the UCSC Genome Browser (Kent et al., 2002). Resultant mapping output files were used as input data for counting the reads per gene using HTseq-count (HTseq Python framework v.0.6.1; parameter: -s no -m union; Anders et al., 2015) and annotation. To determine differentially expressed genes, read counts were introduced into Bioconductor (<http://www.bioconductor.org/>) statistical package DESeq (Anders and Huber, 2010) and edgeR (Robinson et al., 2010) in the R Project for Statistical Computing. OGD and KA samples were compared with their respective controls. P values were corrected for multiple testing using Benjamini-Hochberg (Benjamini and Hochberg, 1995). Genes with corrected P values at ≤ 0.01 were regarded as differentially

expressed. Those differentially expressed in both OGD and KA comparisons were selected for further study.

Transfection of primary neurons

Digested 3×10^6 cortical neurons were resuspended in 100 μ l of nucleofector solution (VPG-1001; Lonza) and mixed with 5 μ g of plasmids. Neurons were then nucleofected using the Amaxa program 0-005 and plated on poly-D-lysine-coated 6-well plates.

shRNA and hGDPGP1 construct

A construct containing a hGDPGP1 ORF (1,158 bp) was purchased from OriGene (RG21252) and subcloned into AAV-CAG-GFP vector for expression in primary neurons (hGDPGP1). Knockdown of GDPGP1 in primary mouse neurons was accomplished using pAAV-U6-GFP vector containing the following target sequences: shGDPGP1 #1, 5'-ACGTCCTTGTGGTGATCAATG-3', and shGDPGP1 #2, 5'-CCGGATTGGAAGTGTTAATT-3'. A construct containing an hGYS1 ORF (2,211 bp) was purchased from OriGene (RG200940) and subcloned into AAV-CAG-GFP vector for expression in primary neurons (hGYS1). Knockdown of GYS1 in primary mouse neurons was achieved using shRNA expression vectors purchased from OriGene (TF509807) containing the following target sequences: shGYS1 #1, 5'-GTGAGCAAACAGTTGTCGCAT TCTTCATC-3', and shGYS1 #2, 5'-GCCTTTCCAGACCACTTC ACCTATGAACC-3'. Scrambled shRNA (shScramble) was used as transfection control.

C. elegans strains

The following strains were used in this work: Punc-47::GFP, Punc-25::GFP, *mcp-1(tm2679)*, *mcp-1(wp38)*, *hif-1(ia4)*, *egl-9(sa307)*, *vhl-1(ok161)*, *hif-1(ia4);vhl-1(ok161)*, *egl-9(sa307);vhl-1(ok161)*, *egl-9(sa307);hif-1(ia4)*, *pfk-1.1(ola72)*, *pfk-1.1(tm5741)*, *mcp-1(tm2679);pfk-1.1(tm5741)*, *pygl-1(tm5211)*, *Pmcp-1::mCherry*, *Pmcp-1::mcp-1*, *Prab-3::mcp-1*, *Pmyo-3::mcp-1*, *Pcol-19::mcp-1*, *Pdpy-7::mcp-1*, *mcp-1(tm2679);Prab-3::mcp-1*, *mcp-1(tm2679);Pmcp-1::mcp-1*, *mcp-1(tm2679);Punc-25::mcp-1*, *mcp-1(tm2679);Pmyo-3::mcp-1*, *mcp-1(tm2679);Pcol-19::mcp-1*, *mcp-1(tm2679);Pdpy-7::mcp-1*, *mcp-1(tm2679);Pspl-1::mcp-1*, *Paex-3::htau*, *Paex-3::htauV337M*, *Paex-3::htauV337M;mcp-1(tm2679)*, *Paex-3::htauV337M;Punc-25::mcp-1*, and *Paex-3::htauV337M;Prab-3::mcp-1*.

Worms were raised on nematode growth medium (NGM) plates at 20°C, using OP50 *Escherichia coli* as a food source (Brenner, 1974). For wild-type nematodes, *C. elegans* Bristol strain N2 was used. Day 1 was defined as 24 h after the final larval stage (L4). The following mutant strains were obtained through the Caenorhabditis Genetics Center: SCL1 (*mcp-1(tm2679)*); DCR3791 (*pfk-1.1(ola72)*); ZG31 (*hif-1(ia4)*); JT307 (*egl-9(sa307)*); and CB5602 (*vhl-1(ok161)*). The Tau model strains *Paex-3::htau* and *Paex-3::htauV337M*, in which wild-type htau (MAPT) or mutant htau carrying the ^{V337M} mutation, respectively, are expressed under the neuron-specific promoter *Paex-3*, were a generous gift from Brian Kraemer (University of Washington, Seattle, WA). *pfk-1.1(tm5741)* strain was provided by the laboratory of Daniel Colón-Ramos (Yale University, New Haven, CT). FX14731 (*pygl-1(tm5211)*) was provided by the MITANI Lab through the National Bio-Resource Project of the Ministry of Education, Culture, Sports, Science and Technology, Japan. To visualize GABA neurons in

regeneration assays, mutants were crossed into *oxIs12* [*Punc-47::GFP*, *lin-15+*] or *julS76* [*Punc-25::GFP*, *lin-15+*] backgrounds.

Expression analysis

For *mcp-1* transcription reporter strains, *Pmcp-1::mCherry* was constructed by combining Gateway (Invitrogen) plasmids encoding the *mcp1* promoter sequence (using a 2,271-bp fragment upstream of the start codon of *mcp-1*), *mCherry*, the *unc-54* UTR sequence, and pCFJ150. *Pmcp-1::mCherry* (10 ng/ μ l) was injected along with the *Pmyo-2::mCherry* coinjection marker (2 ng/ μ l; expressed in the pharynx) into *julS76* [*Punc-25::GFP*, *lin-15+*] animals. Expression was analyzed with an Olympus DSU mounted on an Olympus BX61 microscope, Andor Neo scientific complementary metal-oxide-semiconductor camera, and Lumen light source. Quantification of relative fluorescence was performed by defining a region of interest over GABAergic motor neurons. For both *Punc-25::GFP* (GABA marker) and *Pmcp-1::mCherry* images, the fluorescent intensity was measured using ImageJ (National Institutes of Health). Subsequently, the ratio between *mCherry* and *GFP* signals for a given region of interest was calculated.

CRISPR

The *mcp-1(wp38)* mutant was created by injecting sgRNA targeting *mcp-1* sequence, 5'-GTATCGCCACGAAGTCAATC-3', along with a plasmid encoding Cas9, into N2 wild-type animals (Friedland et al., 2013). The resulting deletion of the fifth and sixth base pair of the first *mcp-1* exon is a frameshift mutation that creates a truncated protein with a premature stop codon after amino acid 41.

Transgenics

The *Punc-25::mcp-1*, *Prab-3::mcp-1*, *Pdpy-7::mcp-1*, *Pcol-19::mcp-1*, and *Pmyo-3::mcp-1* expression vectors were constructed by combining Gateway plasmids encoding the *unc-25*, *rab-3*, *dpy-7*, *col-19*, and *myo-3* promoter sequences, respectively, *mcp-1* coding sequence, the *unc-54* UTR sequence, and pCFJ150. Animals expressing *Punc-25::mcp-1*, *Prab-3::mcp-1*, *Pdpy-7::mcp-1*, *Pcol-19::mcp-1*, *Pmyo-3::mcp-1*, and *Pspl-1::mcp-1* were obtained by injecting wild-type N2 worms with the appropriate expression vector at 10 ng/ μ l, along with *Pmyo-2::mCherry* at 2 ng/ μ l as a coinjection marker and a 1-kb ladder at 50 ng/ μ l as carrier.

C. elegans stress assays

To generate a hypoxic environment, worms on NGM plates were placed in an anaerobic chamber with GasPak EZ Anaerobe Container System Sachets (260001; BD), which produces an anaerobic atmosphere with <1% oxygen within 2.5 h. Unless stated otherwise, hypoxia was applied for 48 h. Survival following hypoxia was determined after 6 h of recovery at 20°C and under normoxic atmosphere. For heat-shock assays, L4 worms were cultured for 6 h at 35°C. Survival of worms was determined after 16 h of recovery at 20°C. Acute exposure to ROS was accomplished by placing worms on 10 mM paraquat-coated plates for 24 h. Worms were scored as dead if not moving spontaneously or after gentle stimulation by repeated pokes on the head and tail with a platinum wire. All experiments were performed on L4-stage worms, unless stated otherwise.

Thrashing assay

L4 worms were transferred to cell culture plates containing M9 buffer to observe their locomotor behavior. Thrashing assays were conducted at room temperature. The number of thrashes was counted for 30 s. A thrash was counted when both the head and tail bent >45° away from the anterior-posterior axis and back again. Approximately 40 worms per strain were used in each thrashing assay.

Lifespan analysis

Lifespan experiments were conducted at 25°C. Newly hatched L1 worms were transferred to NGM plates (day 0) and transferred to new NGM plates every other day. To determine survival of worms under ROS exposure, L1 worms were placed on NGM plates coated with 5 mM paraquat. Worms were scored as dead if they did not move spontaneously or after gentle stimulation by repeated pokes on the head and tail with a platinum wire. Significance was determined with the log rank (Mantel-Cox) test. *n* values were >100 for each condition tested.

Quantification of axonal beadings

The occurrence of axonal beading pathology was analyzed in *juIs76* [*Punc-25:GFP*, *lin-15+*] backgrounds to visualize commissural axons of GABA neurons. Axonal beadings were scored as such if they occupied at least twice the regular axon diameter. Per worm, ≥10 axons were evaluated.

qPCR

To perform quantitative RT-PCR, total RNA was extracted from 100 N2 worms using Qiagen RNeasy. cDNA was made from 100 ng of total RNA with AffinityScript Multiple Temperature cDNA synthesis kit. qPCR was performed with Power SYBR green from Applied Biosystems and cycled on an Applied Biosystems 7500 Fast system. All reactions were repeated multiple times: three technical replicates for each of two biological replicates were performed. No-reverse transcription and no-template controls were included in each experiment. Two to three endogenous controls were included in each experiment, and all data were normalized to actin. *mcp-1* transcript levels in worms were determined using the following primers: 5'-GCC AATGCGGAAATCGTGA-3' (forward) and 5'-TATGGTGCAGAA GACGCAGAAAG-3' (reverse), amplifying a 108-bp fragment spanning exons 2 and 3; actin: 5'-CCCCATCAACCATGAAGATC-3' (forward) and 5'-GACTCGTCGTATTCTTGCTTG-3' (reverse). GDPGP1 transcript levels in primary mouse neurons were determined using the following primers: 5'-TGCCACATCATTTGCAGGAGAC-3' (forward) and 5'-GATGCCTTGTCTTCTCCCAATCC-3' (reverse), amplifying a 71-bp fragment spanning exons 1 and 2; actin: 5'-GCCCTG AGGCTCTTTTCCAG-3' (forward) and 5'-TGCCACAGGATTCCA-TACCC-3' (reverse).

Immunocytochemistry

Immunocytochemistry was performed as described previously (Schulz et al., 2014). Briefly, primary neurons were grown on coverslips and fixed with 4% PFA in PBS for 20 min. After washing in PBS, cells were permeabilized with 0.3% Triton X-100 for 1 min and incubated for 2 h in 1% BSA. Subsequently, cells

were incubated with the primary antibodies at room temperature for 1 h. The following antibodies were used: anti-GDPGP1 (1:100; Novus Biologicals; NBP2-14379) and β III spectrin (1:2,000; Promega; G712A). Following extensive rinsing in PBS, cells were incubated with secondary antibodies linked to Alexa Fluor 488 (1:500, anti-rabbit) or Alexa Fluor 546 (1:500, anti-mouse) for 1 h.

Metabolite assays

Glucose-1-P, glucose-6-P, pyruvate, and glycogen levels in worms and primary mouse neurons were quantified using commercially available kits (ab155892, ab65342, ab83426, and ab65620; Abcam), according to the manufacturer's instructions. For each experiment, 100 L4 worms were transferred to dH₂O (glycogen) or recommended assay buffers, washed, and exposed to repeated freeze-thaw cycles at -80°C to achieve tissue homogenization. Primary neurons (one million cells per 6-well plate and experiment) were washed in cold PBS, lysed in 100 μ l dH₂O (glycogen) or recommended assay buffers, and mechanically homogenized using a 23G syringe. Samples were then boiled for 10 min and centrifuged for 10 min at 18,000 g. The supernatants were used for subsequent colorimetric assays. Absorbances were measured using a microplate reader at recommended wavelengths.

Proteome profiler array

For analyzing the expression profile of cell stress-related proteins in DIV4 primary mouse neurons, Cell Stress Proteome Profiler Array kit (ARY018; R&D Systems) was used per the manufacturer's instructions.

Western blot

Cell lysates were resolved by SDS-PAGE and transferred to nitrocellulose membranes. After incubation in blocking buffer (blocking buffer for fluorescent Western blotting; Rockland; MB-070-010) for 2 h at room temperature, immunoblotting with primary antibodies was performed for 1 h using the following primary antibodies: anti-GDPGP1 (1:500; NBP2-14379; Novus Biologicals) and anti-actin (1:1,000; C4; sc-47778; Santa Cruz). Secondary antibodies (Odyssey IRDye 680 or 800) were also applied for 1 h. Membranes were then washed and visualized using a Licor Odyssey Infrared imaging system. Results were quantified using gel analysis software by ImageJ. Density values were normalized to actin and controls transfections.

Statistical analysis

Comparisons between groups were conducted using an unpaired *t* test, with one-way or two-way ANOVA, if appropriate (GraphPad Prism7). In case of repeated measurements, two-way ANOVA with repeated measures was used. Post hoc comparisons were made with the Holm-Sidak test. Differences were considered significant when *P* < 0.05. All values are presented as means with the corresponding standard errors.

Data availability

The data discussed in this publication have been deposited in NCBI's Gene Expression Omnibus and are accessible through GEO Series accession number GSE111434.

Online supplemental material

Fig. S1 shows that loss of *mcp-1* decreases stress resistance in *C. elegans*. **Fig. S2** shows that *GDPGP1* knockdown in mouse neurons causes up-regulation of stress-related proteins. **Fig. S3** shows that loss of *GDPGP1/mcp-1* does not alter glucose-6-P and pyruvate levels.

Acknowledgments

The skillful and diligent assistance in next-generation sequencing by Ivonne Goerlich and Ivonne Heinze is gratefully acknowledged.

This work was supported by a grant from the Deutsche Forschungsgemeinschaft (SCHU 3039/1-1) to A. Schulz and grants from the National Institutes of Health (R01NS098817 and R01NS094219) to M. Hammarlund. Mutant strains were obtained through the *Caenorhabditis* Genetics Center, which is funded by National Institutes of Health Office of Research Infrastructure Programs (P40 OD010440).

The authors declare no competing financial interests.

Author contributions: A. Schulz conceived and designed the study. M. Hammarlund supervised the experimental program and designed the study. A. Schulz and M. Hammarlund wrote the manuscript. A. Schulz performed the majority of experiments. Y. Sekine performed primary cell culture preparations and transfections thereof. M.J. Oyeyemi performed thrashing assays. S.M. Han, A.J. Abrams, and M. Basavaraju contributed to the generation of *C. elegans* strains used in this study. M. Groth performed RNA-seq and data analysis. H. Morrison contributed to RNA-seq and supervised the experimental program. S.M. Strittmatter supervised the experimental program. All authors approved the final version of the manuscript.

Submitted: 17 July 2018

Revised: 14 October 2019

Accepted: 19 November 2019

References

- Adler, L.N., T.A. Gomez, S.G. Clarke, and C.L. Linster. 2011. A novel GDP-D-glucose phosphorylase involved in quality control of the nucleoside diphosphate sugar pool in *Caenorhabditis elegans* and mammals. *J. Biol. Chem.* 286:21511–21523. <https://doi.org/10.1074/jbc.M111.238774>
- Agostini, M., F. Romeo, S. Inoue, M.V. Niklison-Chirou, A.J. Elia, D. Dinsdale, N. Morone, R.A. Knight, T.W. Mak, and G. Melino. 2016. Metabolic reprogramming during neuronal differentiation. *Cell Death Differ.* 23: 1502–1514. <https://doi.org/10.1038/cdd.2016.36>
- Anders, S., and W. Huber. 2010. Differential expression analysis for sequence count data. *Genome Biol.* 11:R106. <https://doi.org/10.1186/gb-2010-11-10-r106>
- Anders, S., P.T. Pyl, and W. Huber. 2015. HTSeq—a Python framework to work with high-throughput sequencing data. *Bioinformatics.* 31:166–169. <https://doi.org/10.1093/bioinformatics/btu638>
- Beirowski, B., A. N6gr6di, E. Babetto, G. Garcia-alias, and M.P. Coleman. 2010. Mechanisms of axonal spheroid formation in central nervous system Wallerian degeneration. *J. Neuropathol. Exp. Neurol.* 69:455–472. <https://doi.org/10.1097/NEN.0b013e3181da84db>
- Benjamini, Y., and Y. Hochberg. 1995. Controlling the False Discovery Rate: A Practical and Powerful Approach to Multiple Testing. *J. R. Stat. Soc. Series B Stat. Methodol.* 57:289–300.
- Bentley, D.R., S. Balasubramanian, H.P. Swerdlow, G.P. Smith, J. Milton, C.G. Brown, K.P. Hall, D.J. Evers, C.L. Barnes, H.R. Bignell, et al. 2008. Accurate whole human genome sequencing using reversible terminator chemistry. *Nature.* 456:53–59. <https://doi.org/10.1038/nature07517>

- Brenner, S. 1974. The genetics of *Caenorhabditis elegans*. *Genetics.* 77:71–94.
- Camandola, S., and M.P. Mattson. 2017. Brain metabolism in health, aging, and neurodegeneration. *EMBO J.* 36:1474–1492. <https://doi.org/10.15252/embj.201695810>
- Cao, J., J.S. Packer, V. Ramani, D.A. Cusanovich, C. Huynh, R. Daza, X. Qiu, C. Lee, S.N. Furlan, F.J. Steemers, et al. 2017. Comprehensive single-cell transcriptional profiling of a multicellular organism. *Science.* 357: 661–667. <https://doi.org/10.1126/science.aam8940>
- Coleman, M. 2005. Axon degeneration mechanisms: commonality amid diversity. *Nat. Rev. Neurosci.* 6:889–898. <https://doi.org/10.1038/nrn1788>
- Conklin, P.L., S.A. Saracco, S.R. Norris, and R.L. Last. 2000. Identification of ascorbic acid-deficient *Arabidopsis thaliana* mutants. *Genetics.* 154: 847–856.
- De Souza, A.T., X. Dai, A.G. Spencer, T. Reppen, A. Menzie, P.L. Roesch, Y. He, M.J. Caguyong, S. Bloomer, H. Herweijer, et al. 2006. Transcriptional and phenotypic comparisons of Ppara knockout and siRNA knockdown mice. *Nucleic Acids Res.* 34:4486–4494. <https://doi.org/10.1093/nar/gkl609>
- Falkowska, A., I. Gutowska, M. Goschorska, P. Nowacki, D. Chlubek, and I. Baranowska-Bosiacka. 2015. Energy Metabolism of the Brain, Including the Cooperation between Astrocytes and Neurons, Especially in the Context of Glycogen Metabolism. *Int. J. Mol. Sci.* 16:25959–25981. <https://doi.org/10.3390/ijms161125939>
- Friedland, A.E., Y.B. Tzur, K.M. Esvelt, M.P. Colaiacovo, G.M. Church, and J.A. Calarco. 2013. Heritable genome editing in *C. elegans* via a CRISPR-Cas9 system. *Nat. Methods.* 10:741–743. <https://doi.org/10.1038/nmeth.2532>
- Gidday, J.M. 2006. Cerebral preconditioning and ischaemic tolerance. *Nat. Rev. Neurosci.* 7:437–448. <https://doi.org/10.1038/nrn1927>
- Goldberg, M.P., and D.W. Choi. 1993. Combined oxygen and glucose deprivation in cortical cell culture: calcium-dependent and calcium-independent mechanisms of neuronal injury. *J. Neurosci.* 13:3510–3524. <https://doi.org/10.1523/JNEUROSCI.13-08-03510.1993>
- Guthrie, C.R., G.D. Schellenberg, and B.C. Kraemer. 2009. SUT-2 potentiates tau-induced neurotoxicity in *Caenorhabditis elegans*. *Hum. Mol. Genet.* 18:1825–1838. <https://doi.org/10.1093/hmg/ddp099>
- Kent, W.J., C.W. Sugnet, T.S. Furey, K.M. Roskin, T.H. Pringle, A.M. Zahler, and D. Haussler. 2002. The human genome browser at UCSC. *Genome Res.* 12:996–1006. <https://doi.org/10.1101/gr.229102>
- Kraemer, B.C., B. Zhang, J.B. Leverenz, J.H. Thomas, J.Q. Trojanowski, and G.D. Schellenberg. 2003. Neurodegeneration and defective neurotransmission in a *Caenorhabditis elegans* model of tauopathy. *Proc. Natl. Acad. Sci. USA.* 100:9980–9985. <https://doi.org/10.1073/pnas.1533448100>
- LaMacchia, J.C., H.N. Frazier III, and M.B. Roth. 2015. Glycogen Fuels Survival During Hyposmotic-Anoxic Stress in *Caenorhabditis elegans*. *Genetics.* 201:65–74. <https://doi.org/10.1534/genetics.115.179416>
- Majumdar, A.J., W.J. Wong, and M.C. Simon. 2010. Hypoxia-inducible factors and the response to hypoxic stress. *Mol. Cell.* 40:294–309. <https://doi.org/10.1016/j.molcel.2010.09.022>
- Mattson, M.P. 2008. Hormesis defined. *Ageing Res. Rev.* 7:1–7. <https://doi.org/10.1016/j.arr.2007.08.007>
- Nacharaju, P., J. Lewis, C. Easson, S. Yen, J. Hackett, M. Hutton, and S.H. Yen. 1999. Accelerated filament formation from tau protein with specific FTDP-17 missense mutations. *FEBS Lett.* 447:195–199. [https://doi.org/10.1016/S0014-5793\(99\)00294-X](https://doi.org/10.1016/S0014-5793(99)00294-X)
- Robinson, M.D., D.J. McCarthy, and G.K. Smyth. 2010. edgeR: A Bioconductor package for differential expression analysis of digital gene expression data. *Bioinformatics.* 26:139–140. <https://doi.org/10.1093/bioinformatics/btp616>
- Saez, I., J. Duran, C. Sinadinos, A. Beltran, O. Yanes, M.F. Tevy, C. Mart6nez-Pons, M. Mil6n, and J.J. Guinovart. 2014. Neurons have an active glycogen metabolism that contributes to tolerance to hypoxia. *J. Cereb. Blood Flow Metab.* 34:945–955. <https://doi.org/10.1038/jcbfm.2014.33>
- Schulz, A., A. Kyselyova, S.L. Baader, M.J. Jung, A. Zoch, V.F. Mautner, C. Hagel, and H. Morrison. 2014. Neuronal merlin influences ERBB2 receptor expression on Schwann cells through neuregulin 1 type III signalling. *Brain.* 137:420–432. <https://doi.org/10.1093/brain/awt327>
- Scott, B.A., M.S. Avidan, and C.M. Crowder. 2002. Regulation of hypoxic death in *C. elegans* by the insulin/IGF receptor homolog DAF-2. *Science.* 296:2388–2391. <https://doi.org/10.1126/science.1072302>
- Shaye, D.D., and I. Greenwald. 2011. OrthoList: a compendium of *C. elegans* genes with human orthologs. *PLoS One.* 6:e20085. <https://doi.org/10.1371/journal.pone.0020085>
- Taylor, L.M., P.J. McMillan, N.F. Liachko, T.J. Strovos, B. Ghetti, T.D. Bird, C.D. Keene, and B.C. Kraemer. 2018. Pathological phosphorylation of tau and TDP-43 by TTBK1 and TTBK2 drives neurodegeneration. *Mol. Neurodegener.* 13:7. <https://doi.org/10.1186/s13024-018-0237-9>

- Trapnell, C., L. Pachter, and S.L. Salzberg. 2009. TopHat: discovering splice junctions with RNA-Seq. *Bioinformatics*. 25:1105–1111. <https://doi.org/10.1093/bioinformatics/btp120>
- Uhlén, M., L. Fagerberg, B.M. Hallström, C. Lindskog, P. Oksvold, A. Martinoglou, Å. Sivertsson, C. Kampf, E. Sjöstedt, A. Asplund, et al. 2015. Proteomics. Tissue-based map of the human proteome. *Science*. 347: 1260419. <https://doi.org/10.1126/science.1260419>
- Vijayalaxmi, Y.C., Y. Cao, and M.R. Scarfi. 2014. Adaptive response in mammalian cells exposed to non-ionizing radiofrequency fields: A review and gaps in knowledge. *Mutat. Res. Rev. Mutat. Res.* doi:10.1016/j.mrrev.2014.02.002.
- Waitt, A.E., L. Reed, B.R. Ransom, and A.M. Brown. 2017. Emerging Roles for Glycogen in the CNS. *Front. Mol. Neurosci.* 10:73. <https://doi.org/10.3389/fnmol.2017.00073>
- Wang, Q., S. Yu, A. Simonyi, G.Y. Sun, and A.Y. Sun. 2005. Kainic acid-mediated excitotoxicity as a model for neurodegeneration. *Mol. Neurobiol.* 31:3–16. <https://doi.org/10.1385/MN:31:1-3:003>
- Williams, J.A., H.M. Ni, A. Haynes, S. Manley, Y. Li, H. Jaeschke, and W.X. Ding. 2015. Chronic Deletion and Acute Knockdown of Parkin Have Differential Responses to Acetaminophen-induced Mitophagy and Liver Injury in Mice. *J. Biol. Chem.* 290:10934–10946. <https://doi.org/10.1074/jbc.M114.602284>
- Zheng, X., L. Boyer, M. Jin, J. Mertens, Y. Kim, L. Ma, L. Ma, M. Hamm, F.H. Gage, and T. Hunter. 2016. Metabolic reprogramming during neuronal differentiation from aerobic glycolysis to neuronal oxidative phosphorylation. *eLife*. 5:e13374. <https://doi.org/10.7554/eLife.13374>
- Zheng, X.Y., H.L. Zhang, Q. Luo, and J. Zhu. 2011. Kainic acid-induced neurodegenerative model: potentials and limitations. *J. Biomed. Biotechnol.* 2011:457079. <https://doi.org/10.1155/2011/457079>